TRANSIENT PHOTOCURRENT BEHAVIOR IN AMORPHOUS THIN FILM HETEROSTRUCTURES

Oxana Iaseniuc

Institute of Applied Physics, Academiei 5 str., Chisinau, MD-2028 Republic of Moldova

E-mail: oxana.iaseniuc@gmail.com

(Received May 13, 2021)

https://doi.org/10.53081/mjps.2021.20-2.07 CZU:538.9+621.382

Abstract

The characteristics of transient photocurrent in amorphous heterostructures Al–$As_{0.40}S_{0.30}Se_{0.30}$/$Ge_{0.09}As_{0.09}Se_{0.82}$/$Ge_{0.30}As_{0.04}S_{0.66}$–Al in the case of the positive polarity of the applied voltage at the top illuminated Al electrode are presented and discussed in this paper. The complex structure of the spectral distribution of the stationary (Fig. 1) and the transient (Fig. 3) photocurrent characteristics can be assigned to the different values of the optical band gap E_g of the involved amorphous layers (about $E_g \sim 2.0$ eV for $As_{0.40}S_{0.30}Se_{0.30}$ and $Ge_{0.09}As_{0.09}Se_{0.82}$; about $E_g \sim 3.0$ eV for $Ge_{0.30}As_{0.04}S_{0.66}$). It is found that the dependence of photocurrent on light intensity has a power-law behavior $I_{pc} \sim F^{\alpha}$ ($1.0 \leq \alpha \leq 0.5$), which is characteristic of amorphous semiconductors with an exponential distribution of localized states in the band gap.
Keywords: amorphous multilayer structures, photocurrent relaxation, lux–ampere characteristics

Rezumat

În acest articol sunt prezentate și analizate caracteristicile curentului fotoelectric tranzitoriu în heterostructurile amorfe Al–$As_{0.40}S_{0.30}Se_{0.30}$/$Ge_{0.09}As_{0.09}Se_{0.82}$/$Ge_{0.30}As_{0.04}S_{0.66}$–Al pentru cazul aplicarii campului electric de polaritate pozitivă către electrodul din Al de la suprafața iluminat. Structura complexa a curbelor se distribuţie spectrala și a curenților fotoelectrici tranzistorii se datorează a diferitor valori a benziilor optice interzise E_g ale straturilor amorfe componente ($E_g \sim 2.0$ eV pentru $As_{0.40}S_{0.30}Se_{0.30}$ și $Ge_{0.09}As_{0.09}Se_{0.82}$, și $E_g \sim 3.0$ eV pentru $Ge_{0.30}As_{0.04}S_{0.66}$). A fost stabilit, că dependența curentului fotoelectric de intensitatea luminii se caracterizeaza conform unei dependențe cu caracter de putere $I_{pc} \sim F^{\alpha}$ ($1.0 \leq \alpha \leq 0.5$), si care este caracteristică pentru semiconductori amorfi cu distribuția exponențială a stărilor localizate în banda interzisă de energie.
Cuvinte cheie: structuri multistrat amorfe, relaxare fotocurentă, caracteristici lux-ampere

1. Introduction

Ternary glasses As–S–Se, Ge–As–Se, and Ge–As–S attract attention due to their wide potential application in IR optics, non-linear optics, photonics, and optoelectronics and as

registration media for holography [1–3] and e-beam lithography [4–6]. It is well known that the functionality of many photonic and optoelectronic devices is based on the intrinsic photoelectric effect. The photocurrent spectra and the kinetics of the photocurrent can give information regarding the mechanisms of generation, recombination and drift processes of non-equilibrium carriers in amorphous materials. From this point of view, studies of the stationary and transient characteristics of photoconductivity of ternary amorphous thin films and multilayer structures (heterostructures) can give additional information about these processes and therefore can present a special interest. Moreover, recently, some studies focused on multilayered amorphous thin film structures, which have an advantage over single-layer structures, have been published [7–11]. It has been found that the predominant mechanisms of recombination of photo-excited carriers in the studied amorphous materials are mono- and bimolecular and the transport is controlled by the multiple trapping processes with an exponential distribution of the localized states in the band gap [12–14].

2. Experimental

Bulk chalcogenide glasses $As_{0.40}S_{0.30}Se_{0.30}$, $Ge_{0.09}As_{0.09}Se_{0.82}$, and $Ge_{0.30}As_{0.04}S_{0.66}$ were prepared from the elements of the *6N* purity (Ge, As, S, Se) by a conventional melt quenching method. The initial materials were weighed, batched into quartz tubes, and sealed in a vacuum of $P = 10^{-5}$ Torr. After sealing, the tubes were heated at a temperature of about $T = 1000^{o}$C for 48 h. After that, the homogenized melt-containing tubes were air-quenched to room temperature. Some glass samples were cut and polished for optical measurements (IR spectrophotometer); the other samples were prepared as small granules for vacuum evaporation.

Thin film samples of each amorphous material with a thickness of about $d = 1000$ nm for $As_{0.40}S_{0.30}Se_{0.30}$, $d = 500$ nm for $Ge_{0.09}As_{0.09}Se_{0.82}$, and $d = 200$ nm for $Ge_{0.30}As_{0.04}S_{0.66}$ with Al-electrodes were prepared by thermal evaporation in a vacuum ($P = 10^{-5}$ Torr) onto glass substrates for photoelectrical measurements. The thickness of each layer was chosen from considerations of the resistance of the layer to provide a uniform distribution of the applied electrical field in each layer of the multilayer structures. The transparency of the top Al-electrode for the incident light was about 60–70 %; the area of the samples was about $S = 0.5$ cm^2. Multilayer heterostructures (HS) Al–$As_{0.40}S_{0.30}Se_{0.30}$/$Ge_{0.09}As_{0.09}Se_{0.82}$/$Ge_{0.30}As_{0.04}S_{0.66}$–Al were prepared in the same technological cycle; they had a sandwich configuration with two Al-electrodes. The spectral distribution of stationary photocurrent $Ipc = f(\lambda)$ was registered under constant current conditions using an SPM-2 spectrophotometer and a U1-7 electrometrical amplifier with the error less than ±1.0 %. All experiments were performed at room temperature ($T \approx 20$°C).

3. Results and Discussion

The steady-state photoconductivity spectra of all the amorphous thin film structures were registered at an external electric field of $E = 5 \times 10^4$ V/cm^2 (plus polarity on the top Al illuminated electrode); e.g., *I–V* characteristics exhibiting an appropriate linear behavior were recorded in the region [10].

Figure 1 shows the steady-state photocurrent spectra of separate amorphous thin films and HS Al–$As_{0.40}S_{0.30}Se_{0.30}$/$Ge_{0.09}As_{0.09}Se_{0.82}$/$Ge_{.0.30}As_{0.04}S_{0.66}$–Al at a positive voltage applied to the

top illuminated Al electrode ($E = 5 \times 10^4$ V/cm^2). The steady-state photocurrent spectra show that the position of the maximum photocurrent of the component layers of the multilayer HS are in good agreement with the absorption spectra [10]. The photocurrent spectra are governed by the different value of the optical band gap of the involved amorphous layer (about $E_g \sim 2.0$ eV for $As_{0.40}S_{0.30}Se_{0.30}$ and $Ge_{0.09}As_{0.09}Se_{0.82}$; about $E_g \sim 3.0$ eV for $Ge_{0.30}As_{0.04}S_{0.66}$).

The maximum photocurrent is recorded at λ = 0.54 μm ($h\nu$ = 2.30 eV) for the Al–$As_{0.40}Se_{0.30}S_{0.30}$–Al thin film structure, at λ = 0.50 μm ($h\nu$ = 2.47 eV) for the Al–$Ge_{0.09}As_{0.09}Se_{0.82}$–Al, and at λ = 0.42 μm ($h\nu$ = 2.95 eV) for the Al–$Ge_{0.30}As_{0.04}S_{0.66}$–Al with an additional maximum at λ = 0.51 μm ($h\nu$ = 2.42 eV), respectively. It was found that the position of these maxima do not depend on the polarity of the applied voltage. The spectral distribution of the photocurrent for the HS is recorded in the intermediate region at λ = 0.44 μm ($h\nu$ = 2.82 eV) between the positions of the separate layers.

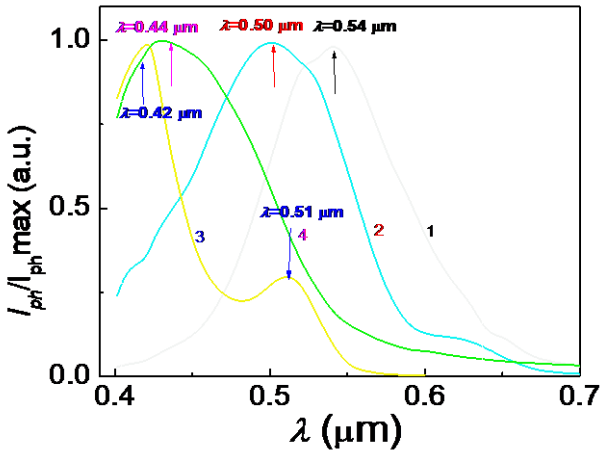

Fig. 1. Spectral characteristics of photocurrent for amorphous structures: (*1*) Al–$As_{0.40}Se_{0.30}S_{0.30}$–Al, (*2*) Al–$Ge_{0.09}As_{0.09}Se_{0.82}$–Al, (*3*) Al–$Ge_{0.30}As_{0.04}S_{0.66}$–Al, and (*4*) Al–HS–Al. Applied field: $E = 5 \times 10^4$ V/cm^2.

Figure 2 shows the photocurrent relaxation curves for amorphous HS Al–$As_{0.40}S_{0.30}Se_{0.30}$/$Ge_{0.09}As_{0.09}Se_{0.82}$/$Ge_{0.30}As_{0.04}S_{0.66}$–Al at different light intensities *F* of (*1*) 1.5, (*2*) 6.5, (*3*) 15, (*4*) 72, and (*5*) 199%at a wavelength excitation of λ_{exc} = 0.56 μm and an applied voltage of *U* = ”+” 10 V to the top illuminated Al electrode. It was observed that, at low light intensities, the steady-state values of the photocurrent reach a stationary state without passing through the maximum (curve *1*). At higher intensities, the relaxation curves exhibit a maximum (so-called “spike”); after that, the photocurrent relaxes to stationary values (curves *2*–*5*). With an increase in the light intensity, the amplitude of the “spike” also increases.

The experiments on studying the time characteristics of the transient photocurrent were performed at different light intensities (Fig. 2) and wavelengths (Fig. 3). A photo-shutter was used to switch the light on/off. The experimental data were acquired in the digital form using the Arduino electronics platform based on hardware and software.

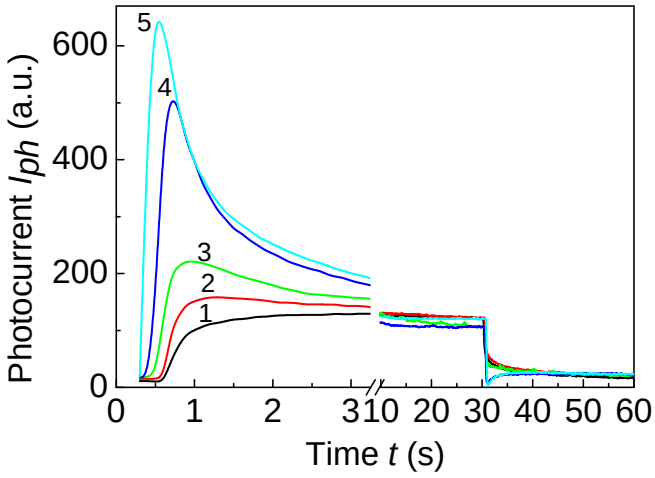

Fig. 2. Photocurrent relaxation curves for amorphous HS Al–$As_{0.40}S_{0.30}Se_{0.30}$/$Ge_{0.09}As_{0.09}Se_{0.82}$/$Ge_{0.30}As_{0.04}S_{0.66}$–Al at different light intensities *F* of (*1*) 1.5, (*2*) 6.5, (*3*) 15, (*4*) 72, and (*5*) 100%; λ_{exc} = 0.56 μm, *U* = "+" 10 V applied to the top illuminated Al electrode.

Figure 2 shows that, after switching the illumination off, at high intensities, the decay portions of the photocurrent curves exhibit some anomalies, the photocurrent drops below its stationary value. This phenomenon can be interpreted in terms of the contact phenomenon that appears between the contacts of the metallic electrode with the amorphous materials and between the interfaces of the two amorphous layers [12, Chapter 9]. The maximum light intensity *F* at an excitation wavelength of λ = 560 nm was $F = 10^{16}$ photons/cm^2, which corresponds to *F* in the respective curves in Fig. 2: (*1*) 1.5×10^{14}, (*2*) 6.5×10^{14}, (*3*) 1.5×10^{15}, (*4*) 7.2×10^{15}, and (*5*) 1×10^{16} photons/cm^2.

Figure 3 shows the photocurrent relaxation curves for amorphous HS Al–$As_{0.40}S_{0.30}Se_{0.30}$/$Ge_{0.09}As_{0.09}Se_{0.82}$/$Ge_{0.30}As_{0.04}S_{0.66}$–Al at different wavelengths and an excitation with maximum light emission intensity at a voltage of *U* = +10 V applied to the top illuminated Al electrode. With a decrease in the photon energy $h\nu$ in the region of maximum photosensitivity, the photocurrent also reaches a stationary value passing through the maximum. Curve *3* shows the relaxation of the photocurrent for the maximum photocurrent value in the spectral distribution of the photocurrent (see Fig. 1).

Figure 4 shows the dependence of the maximum photocurrent ("spike") on light intensity $\mathrm{Log}(I_{phc}) = f(\mathrm{Log}F)$ (lux–ampere characteristics) for amorphous HS Al–$As_{0.40}S_{0.30}Se_{0.30}$/$Ge_{0.09}As_{0.09}Se_{0.82}$/$Ge_{0.30}As_{0.04}S_{0.66}$–Al at a maximum of wavelength λ = 0.560 μm. It was found that this dependence is nonlinear; in the case of an exponential distribution of localized states in the band gap of the amorphous material, it is described by the following expression: $I_{pc} \sim F^{\alpha}$, were α (power index) takes values of $0.5 \le \alpha = \dfrac{T^*}{T+T^*} \le 1.0$, where T^* is the parameter of the localized state distribution [12]. In our case, the calculated T^* parameter for the studied amorphous structure takes a value of T^* = 342 K, which is in good agreement with that for the other amorphous semiconductors.

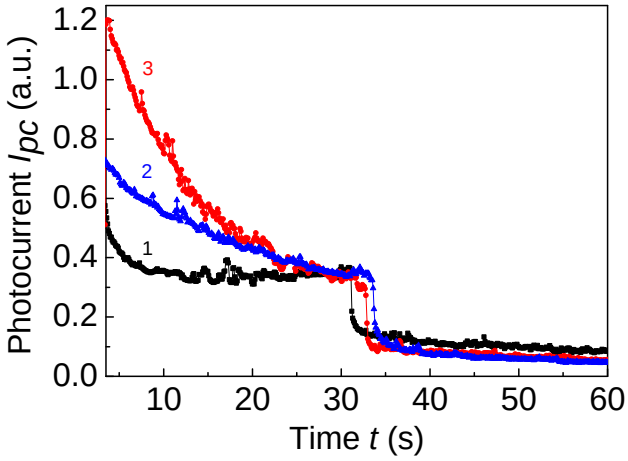

Fig. 3. Photocurrent relaxation curves for amorphous HS Al–$As_{0.40}S_{0.30}Se_{0.30}$/$Ge_{0.09}As_{0.09}Se_{0.82}$/$Ge_{0.30}As_{0.04}S_{0.66}$–Al at the different wavelengths λ of (*1*) 0.500, (*2*) 0.560, and (*3*) 0.630 μm; *U* = "+" 10 V is applied to the top illuminated Al electrode.

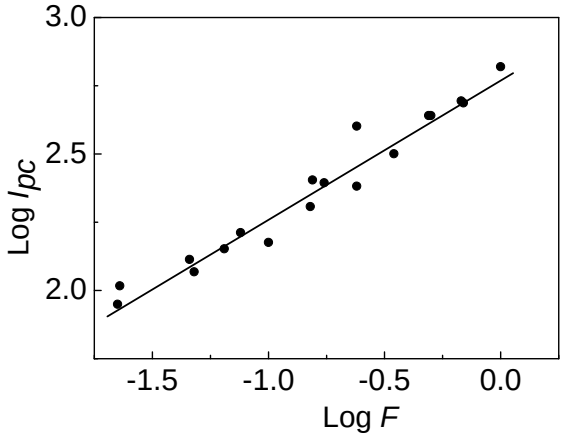

Fig. 4. Dependence of the photocurrent Log(I_{phc}) = *f*(Log*F*) for amorphous HS Al–$As_{0.40}S_{0.30}Se_{0.30}$/$Ge_{0.09}As_{0.09}Se_{0.82}$/$Ge_{0.30}As_{0.04}S_{0.66}$–Al at a wavelength of λ = 0.560 μm and *U* of "+" 10 V applied to the top illuminated Al electrode.

Photoconductivity relaxation in amorphous chalcogenides is satisfactorily interpreted within the framework of the model of multiple trapping of states quasi-continuously distributed in the mobility gap of the amorphous semiconductors by the band gap [13–15]. The application of this model provides a better understanding of some other non-equilibrium processes specific only for chalcogenide glassy semiconductors, such as dispersive transport and induced optical absorption, in particular, the transients between steady states. Analysis of these processes leads to the conclusion about the exponential form of the energy distribution *N(E)* of the localized state density as follows:

$$N(E) = (Nt/kT^*) \exp(-E/kT^*), \quad (1)$$

where N_t is the total gap-state density.
Under standard simplifying assumptions, the relation between the state density $N(E)$ and absorption spectrum $\alpha(h\nu)$ takes the form

$$N(E_c - h\nu) = M[d\alpha/d(h\nu)], \quad (2)$$

where $M \approx 10^{17}$ cm^{-2} [16].

The state density N calculated from the differentiation of $\alpha(h\nu)$ and represented in the photoconductivity spectra gives a value of $N = 5 \times 10^{17}$ cm^{-3} eV^{-1}, which it is in good agreement with the values determined for vitreous As_2S_3 [17]. The absorption coefficient $\alpha(h\nu)$ is determined by the optical transitions from the filled localized states to the free states in the conduction band. The dipole matrix element of the transition does not depend on the excitation energy, and the distribution of delocalized states is approximated by a step function.

The theoretical consideration of the photocurrent relaxation in terms of the multiple trapping model with energy states exponentially distributed in band gap allows revealing several definite time domains in transient photocurrent curves. Each of these domains corresponds to a power dependence of photocurrent upon time and is determined by the capture of free carriers in traps or by their recombination in monomolecular or bimolecular regimes.

The absence of a "spike" in the ascending portions of the photocurrent in amorphous HS Al–$As_{0.40}S_{0.30}Se_{0.30}$/$Ge_{0.09}As_{0.09}Se_{0.82}$/$Ge_{0.30}As_{0.04}S_{0.66}$–Al at low light intensities indicates that the capture of non-equilibrium carriers is intensified, since the generation of the photocurrent is balanced by the capture, rather than by its recombination. Conversely, at higher light intensities, the presence of a "spike" in the ascending portions of the photocurrent indicates that the bimolecular recombination process rate is higher than the capture rate. It is shown that the photocurrent decay rate abruptly increases with an increasein the light intensity. The non-equilibrium relaxation of the photocurrent is typical for the majority of amorphous semiconductors; it is usually attributed to the wide spectrum of the localized states in a mobility gap. For the amorphous As_2S_3 and As_2S_3:Pr films, it was found that, after switching the light off, the photocurrent decay occurs, initially due to the capture of non-equilibrium charge carriers by the band tail of localized states and subsequently due to their recombination [15].

4. Conclusions

The experimental results on transient photocurrents in multilayer HS Al–$As_{0.40}S_{0.30}Se_{0.30}$/$Ge_{0.09}As_{0.09}Se_{0.82}$/$Ge_{0.30}As_{0.04}S_{0.66}$–Al at different light intensities and wavelengths have been described and discussed. The experimental results have been interpreted taking into account the contact phenomena between the metal and the amorphous semiconductor and the drift of non-equilibrium carriers through the sample.

It has been found that the dependence of the photocurrent on light intensity exhibits a power-law behavior $I_{ph} \sim F^{\alpha}$ ($1.0 \le \alpha \le 0.5$; $\alpha = 0.6$; characteristic temperature, $T^* = 342$ K), which is characteristic of amorphous semiconductors with an exponential distribution of the localized states in the band gap. At photon energies of $h\nu \ge E_g$ and high light intensities, the ascending portion of the relaxation curves of the photocurrent exhibits a "spike", which is

quenched at higher wavelengths and low light intensities. It has been found that the photocurrent relaxation in the amorphous thin films is consistent with the model of trap-controlled capture with traps exponentially distributed in the band gap.

The obtained experimental results have been discussed taking into account the depth of the light absorption depending of the nature and thickness of each amorphous material, the wavelength, and the contact phenomena at the interfaces of the different materials and the metal–amorphous semiconductor interfaces with different work functions, as was shown for other amorphous thin film structures.

Acknowledgements. This work was supported by the ANCD 20.80009.5007.14 project. The author thanks Prof. M. Iovu for helpful discussions.

References

[1] A. Chirita, T. Galstean, M. Caraman, O. Korshak, and V. Prilepov, Optoelectron. Adv. Mater. Rapid Commun. 7, 293 (2013).
[2] A. Chirita, V. Prilepov, M. Popescu, I. Andries, M. Caraman, and Iu. Jidcov, J. Optoelectron. Adv. Mater. 17, 925 (2015).
[3] A. Chirita, V. Prilepov, M. Popescu, O. Corsac, P. Chetrus, and N. Nasedchina, Optoelectron. Adv. Mater. Rapid Commun. 9, 919 (2015).
[4] I. Blonskyi, V. Kadan, O. Shpotytuk, M. Iovu, P. Korenyuk, and I. Dmitruk, Appl. Phys. B 104, 951 (2011).
[5] M. Reinfelde and J. Teteris, J. Optoelectron. Adv. Mater. 13(11–12), 1531 (2011).
[6] S. A. Sergeev, M. S. Iovu, and A. Yu. Meshalkin, Chalcogenide Lett. 17(1), 25 (2020).
[7] A. Kikineshi, V. Polyok, I. A. Szabo, M. Shipljak, I. Ivan, and D. L. Beke, J. Non-Cryst. Solids 326, 484 (2003).
[8] M. L. Trunov, P. M. Nagy, V. Takats, P. M. Lytvyn, S. Kokenesi, and E. Kalman, J. Non-Cryst. Solids 355, 1993 (2009).
[9] O. V. Iaseniuc and M.S. Iovu, in Proc. SPIE, vol. 11718 (2020).
[10] O. Iaseniuc and M. Iovu, Beilstein J. Nanotechnol. 11, 1757 (2020).
[11] O. Iaseniuc and M. Iovu, Proc. Rom. Acad., Ser. A 21(3), 231 (2020).
[12] M. Popescu, A. Andrieș, V. Ciumaș, M. Iovu, S. Șutov, and D. Țiuleanu, Physics of Chalcogenide Glasses, Stiinta, Chisinau, 1996.
[13] V. I. Arkhipov, M. S. Iovu, A. I. Rudenko, and S. D. Shutov, Sov. Phys. Semicond. 19(1), 101 (1985).
[14] V. I. Arkipov, M. S. Iovu, A.I. Rudenko, and S. D. Shutov, Solid State Commun. 62(5), 3391 (987).
[15] M. S. Iovu, I. A. Vasiliev, E. P. Colomeico, E. V. Emelianova, V. I. Arkhipov, and G. J. Adriaenssens, J. Phys: Condens. Matter. 16 (17), 2949 (2004).
[16] M. S. Iovu and O. V. Iaseniuc, Optoelectron. Adv. Mater. Rapid Commun. 12(9–10), 563 (2018).
[17] M. S. Iovu, S. D. Shutov, A. M. Andriesh, E. I. Kamitsos, C. P. E. Varsamis, D. Furniss, A. B. Seddon, and M. Popescu, J. Optoelectron. Adv. Mater. 3(2), 443 (2001).